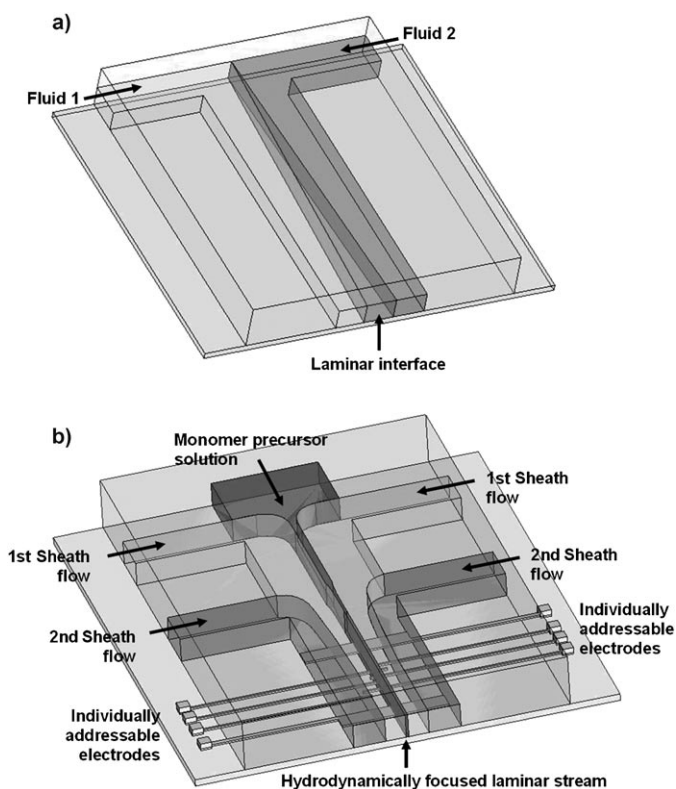


# A Hydrodynamically Focused Stream as a Dynamic Template for Site-Specific Electrochemical Micropatterning of Conducting Polymers\*\*

Shuang Hou, Shutao Wang, Zeta T. F. Yu, Nicole Q. M. Zhu, Kan Liu, Jing Sun, Wei-Yu Lin, Clifton K.-F. Shen, Xiaohong Fang,\* and Hsian-Rong Tseng\*

Micropatterning technology<sup>[1–3]</sup> has been a major driving force behind the development of organic microelectronic devices. There have been significant efforts devoted to exploring this technology for the fabrication of conducting polymer (CP)-based devices in particular, because CPs<sup>[4–6]</sup> exhibit the unique advantages of tunable conductance, chemical specificity, flexible modification, and low fabrication cost. In general, most of the existing micropatterning approaches,<sup>[1–3]</sup> for example, the embossing method,<sup>[7]</sup> imprint lithography,<sup>[8]</sup> capillary molding,<sup>[9,10]</sup> and microcontact printing,<sup>[11,12]</sup> require the use of prefabricated solid molds or templates to determine the features and dimensions of the micropatterns. These molds and templates are normally fabricated by lithographic means, so their embedded features are very much fixed and it is unlikely that they would be reprogrammed for different micropattern features.

Alternatively, an emerging set of micropatterning approaches, which utilize spatially defined laminar interfaces as flowing templates, have been developed.<sup>[13–15]</sup> In these cases (Figure 1 a), two miscible fluid streams were introduced into a microfluidic channel to generate a distinct flow interface<sup>[16,17]</sup> between the adjacent laminar streams. As the small lengths of the microchannels impart a low Reynolds number ( $Re < 2000$ ) to the microfluidic system, the dimension of the resulting laminar interface is kinetically stable and sharply defined. Specific chemical reactions that generate insoluble materials can therefore be confined in these flowing tem-



**Figure 1.** a) A laminar interface generated between two miscible fluid streams can serve as a flowing template for continuous micropatterning in a fluidic channel. b) A hydrodynamically focused laminar stream produced in a new type of microfluidic setup can be employed as a dynamic template for site-specific electrochemical deposition of size-controllable CP micropatterns across individually addressable electrode junction pairs.

[\*] S. Hou,<sup>[‡]</sup> Prof. X. Fang

Key Laboratory of Molecular Nanostructure and Nanotechnology  
Beijing National Laboratory for Molecular Sciences  
Institute of Chemistry, Chinese Academy of Sciences  
2 North 1st St., Zhongguancun, Beijing 100080 (China)  
Fax: (+86) 10-6265-0024  
E-mail: xfang@iccas.ac.cn

S. Hou,<sup>[‡]</sup> Dr. S. Wang,<sup>[‡]</sup> Z. T. F. Yu, N. Q. M. Zhu, Dr. K. Liu,  
Dr. J. Sun, Dr. W.-Y. Lin, Dr. C. K.-F. Shen, Prof. H.-R. Tseng  
Crump Institute for Molecular Imaging  
Department of Molecular and Medical Pharmacology  
David Geffen School of Medicine at UCLA  
700 Westwood Plaza, Los Angeles, CA 90095 (USA)  
Fax: (+1) 310-206-8975  
E-mail: hrtseng@mednet.ucla.edu  
Homepage: <http://labs.pharmacology.ucla.edu/tsenglab/>

[‡] These two authors contributed equally to this work.

[\*\*] This research was supported by the DOD-Defense Threat Reduction Agency (W911NF0610243), the NIH-NCI NanoSystems Biology Cancer Center (U54A119347), and the National Nature Science Foundation of China (No. 90406006).



Supporting information for this article is available on the WWW under <http://www.angewandte.org> or from the author.

plates (that is, laminar interfaces) for in situ deposition<sup>[13–15]</sup> of continuous micropatterns in the microchannels.

Herein, we introduce a new type of micropatterning approach in a microfluidic setting (Figure 1 b), in which a hydrodynamically focused laminar stream<sup>[18]</sup> was generated in situ for performing size-controllable, site-specific electrochemical deposition of CP micropatterns across individually addressable electrode junction pairs. Although the previously developed laminar-interface-templated micropatterning method<sup>[13–15]</sup> shares a similar concept, it is unlikely to employ this method for size-controllable, site-specific micropatterning because of the intrinsic limitations associated with the diffusion-controlled interface dimensions<sup>[16,17]</sup> and the continuous reaction/deposition processes.<sup>[13–15]</sup>

Our hydrodynamically focused stream-templated micropatterning approach is developed to overcome these limitations. By using a microfluidic device with multiple micro-channel inlets (Figure 1b), a focused stream can be produced. The width of the focused stream can be altered by changing the flow rates of the surrounding sheath streams, and the position (parallel to the flow direction) of the focused stream can be altered by the ratio of the sheath flow rates applied on both sides of the focused stream. By combining the dynamic characteristics of the flow with the size and position controllability, such a focused stream is defined as a dynamic template that allows arbitrary spatial confinement of the redox-active monomer precursors for electrochemical micropatterning.

More importantly, the deposition of a micropattern will not occur until an effective electrochemical potential is applied at the electrode junction located underneath the focused stream. Using this microfluidic setup, we have successfully demonstrated the site-specific fabrication of an array of polypyrrole (Ppy) micropatterns with controllable widths ranging from 1 to 5  $\mu\text{m}$ . We also validated the fabrication fidelity and device scalability of this micropatterning approach by fabricating a sensor array composed of two different types of CP micropattern electrode junctions, that is, seven Ppy and six carboxylic acid-substituted Ppy (COOH-Ppy) junctions in a monolithic device. Two different sensing elements, a Ppy and a COOH-Ppy micropattern electrode junction, selected from the sensor array were utilized to test the concept of an electronic nose.<sup>[19–21]</sup> We were able to distinguish a library of saturated organic solvent vapors with this binary resistive sensor.

The microfluidic device (Figure 2a) is composed of 1) an array of 20 electrode junctions on a glass substrate (with three different types of junction gaps of 2, 4, and 10  $\mu\text{m}$ ) for electrochemical deposition of CP micropatterns and 2) an overlaying polydimethylsiloxane component (with embedded 200- $\mu\text{m}$ -wide and 40- $\mu\text{m}$ -high microchannels) for hydrodynamic focusing of the monomeric precursor (that is, pyrrole and its derivative) solution. These two components were fabricated separately by standard photolithography<sup>[22,23]</sup> and soft lithography<sup>[24]</sup> and then bonded together after oxygen plasma treatment.<sup>[25,26]</sup>

For fluid delivery, syringes and syringe pumps were used to deliver the pyrrole solution (0.1M pyrrole, 0.1M  $\text{LiClO}_4$ , and 1.0 mM HCl) into the microfluidic channel at a constant flow rate (1.0  $\mu\text{L min}^{-1}$ ), while the sheath streams (18 M $\Omega$  water) were at variable flow rates ranging from 2.5 to 60  $\mu\text{L min}^{-1}$ . As shown in Figure 2b, the pyrrole solution was first introduced into the device through the central inlet, and two pairs of sheath streams were then employed to compress the pyrrole solution, which resulted in a hydrodynamically focused

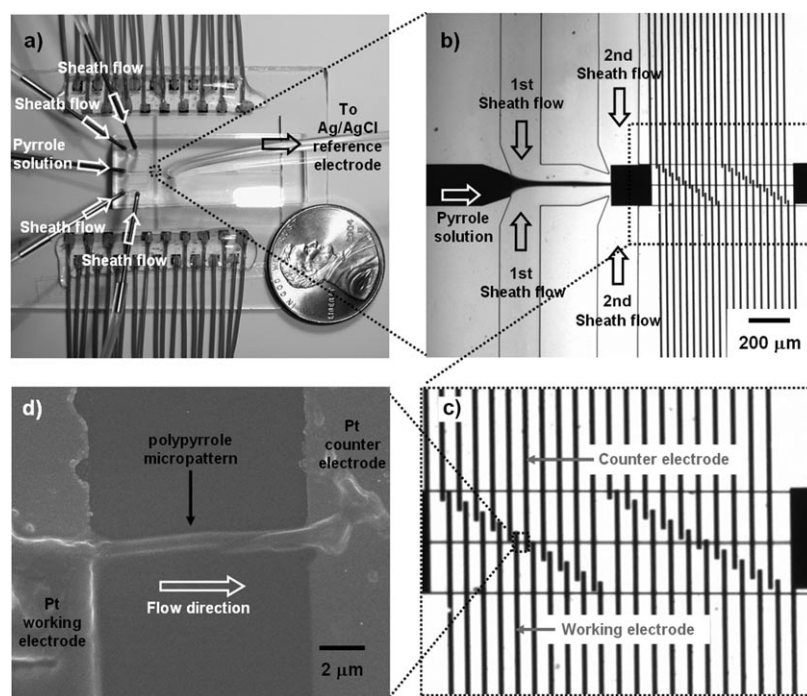


**Figure 2.** a) Photograph of the actual microfluidic device. b) Micrograph of the device in action. A pyrrole solution (flow rate: 1.0  $\mu\text{L min}^{-1}$ ) was first injected into the device, and two pairs of sheath streams (flow rate: 30  $\mu\text{L min}^{-1}$ ) were employed to compress the pyrrole solution in sequence to generate a 2- $\mu\text{m}$ -wide hydrodynamically focused laminar stream. To help visualize the flow characteristics, food dye was dissolved in the pyrrole solution. c) The 2- $\mu\text{m}$ -wide focused laminar stream served as a dynamic template for deposition of a 1- $\mu\text{m}$ -wide Ppy micropattern across a 10- $\mu\text{m}$  microelectrode junction gap where a constant current (200 nA) was applied. d) Scanning electron microscopy (SEM) image of the 1- $\mu\text{m}$ -wide Ppy micropattern across a Pt electrode pair.

laminar stream. Again, the width and position of the resulting focused stream were controllable by the flow rates of the surrounding sheath streams. Importantly, the use of two-step sheath-stream compression conferred an improved stability to the focused stream, in contrast to that observed in a one-step hydrodynamic focusing setup, especially when the focused beam width was less than 4  $\mu\text{m}$ .<sup>[27]</sup>

To help visualize the diffusion broadening of the focused beam, a fluorescent solution containing 5-carboxyfluorescein (10 nM) was used to replace the pyrrole solution in the hydrodynamic focusing experiment, and fluorescence microscopy (see the Supporting Information) was employed to characterize the diffusion broadening of the resulting fluorescent focused stream. The results indicated that the diffusion broadening is negligible<sup>[18]</sup> because of the extremely short retention time of the focused beam generated in situ, as a result of its high speed (0.042 to 0.252  $\text{ms}^{-1}$ ) and short traveling distance (100 to 1000  $\mu\text{m}$  downstream of the final focused point). In the electrochemical setup, the working and counter electrodes of a standard three-electrode configuration were connected to an adjacent electrode pair (Figure 2c), and the reference outlet was linked to an Ag/AgCl microelectrode located at the end of the outlet tubing (Figure 2a).

Initially, pyrrole-containing laminar streams with focused stream widths of 2, 5, and 10  $\mu\text{m}$  were generated as dynamic templates for growing Ppy micropatterns (Figure 2d) across

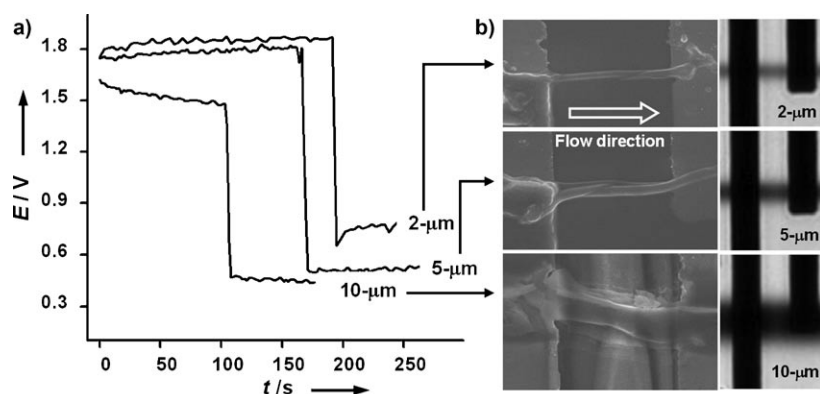


**Figure 3.** a) Plots of potential ( $E$ ) versus time ( $t$ ) for electrochemical deposition of Ppy micropatterns across the respective 10- $\mu\text{m}$  electrode gaps in the presence of 2, 5, and 10- $\mu\text{m}$ -wide focused streams. b) Optical micrographs (right) of the applied focused streams and SEM images (left) of the resulting Ppy micropatterns.

the 10- $\mu\text{m}$  junction gaps, by a galvanostatic method (Figure 3) at current intensities of 200, 400, and 800 nA, respectively. In this microfluidic system, we observed consistent deposition times of approximately 100–250 s and relatively higher electrochemical potentials ranging from 1.3 to 1.6 V compared to those reported in the regular electrochemical setup (ca. 1.1 V).<sup>[28,29]</sup> The SEM images shown in Figure 3 reveal that the 1-, 2-, and 5- $\mu\text{m}$ -wide micropatterns were grown across the 10- $\mu\text{m}$  junction gaps in the presence of 2, 5, and 10- $\mu\text{m}$ -wide focused streams, respectively. A profilometer was used to examine the micropatterns and gave their vertical profiles in the ranges of 100–250, 340–600, and 1000–1200 nm, respectively.

Notably, the electrochemical setup allows self-regulated growth of micropatterns. When the micropatterns were grown across the electrode junctions, the electrochemical deposition slowed down dramatically as a result of the reduction of overall resistance. As a result of the use of transparent substrates (glass slides), the growing process of the micropatterns could be visualized in real time by an inverted optical microscope (see movie clip in the Supporting Information). Out of more than 200 studies, our results suggest that the experimental fidelity was affected by the widths of the focused stream employed in the micropatterning process. When the focused streams were  $> 5 \mu\text{m}$ , 95 % of the device yield was achieved. This yield dropped to 70 % in the presence of 2- $\mu\text{m}$ -wide focused streams. Although we were able to grow Ppy nanopatterns using focused streams with widths  $< 1 \mu\text{m}$ , a low device yield (20 %) was obtained.

On account of the easy modification feature of CPs, a variety of functional groups can be introduced into individual CP micropatterns by site-specific electrochemical polymerization of the respective monomeric precursors. With this idea in mind, we introduced carboxylic acid-substituted pyrrole<sup>[30]</sup> (that is, a mixture of pyrrole and COOH-substituted pyrrole in a molar ratio of 1:5) into the 2- $\mu\text{m}$ -wide focused streams for depositing the COOH-Ppy micropattern junctions using the electrochemical conditions described above. Compared to the Ppy micropattern junctions, the COOH-Ppy junctions exhibited a two-order increase in conductance, which can be

attributed to the doping effect associated with carboxylic acid groups.

Subsequently, we were able to carry out site-specific depositions of seven Ppy and six COOH-Ppy micropatterns at different electrode junction pairs in the same device. The resulting microfluidic device with embedded Ppy and COOH-Ppy micropattern junctions provides a ready-to-use sensor array capable of handling and detecting extremely small quantities of chemical analytes. Two sensing elements (one Ppy and one COOH-Ppy) were randomly selected from the 13 functioning micropattern junctions to act as a binary sensor. Using a custom-designed setup (see the Supporting Information), we demonstrated that this binary sensor was able to respond specifically (Figure 4a) to a collection of 12 organic vapors (20  $\mu\text{L}$  each).

A scatter plot (Figure 4b) summarizes the resistive responses of this binary sensor to the 12 organic vapors. The

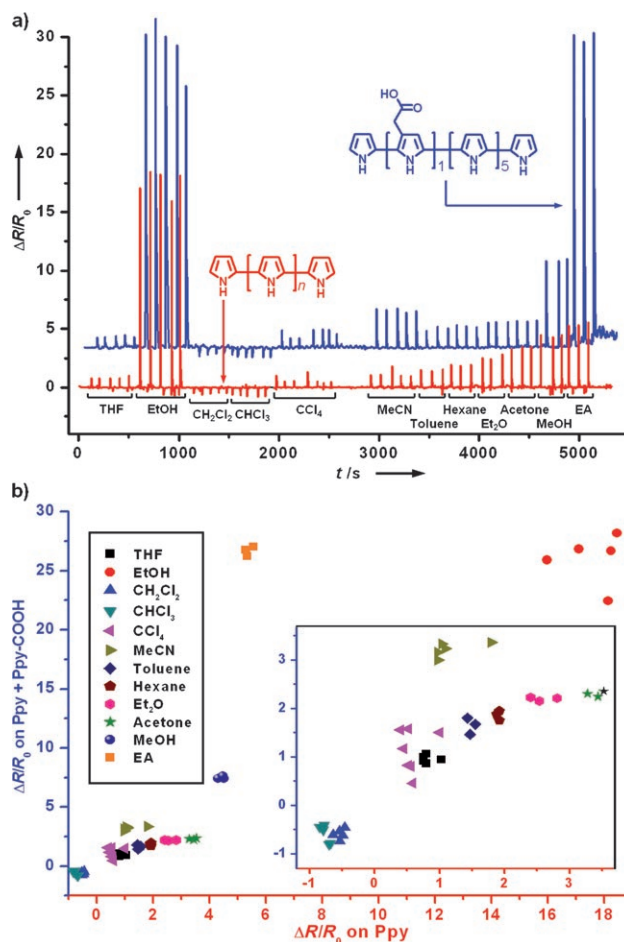


**Figure 4.** a) Real-time resistance responses ( $R$ ) of a binary sensor composed of a Ppy- and a COOH-Ppy-based micropattern electrode junction upon periodic exposure to a library of saturated organic vapors (each 20  $\mu\text{L}$  in volume). b) Scatter plot summarizing the collective sensing responses to individual organic vapors. EA = ethyl acetate.



horizontal and vertical axes represent the specific resistive responses ( $\Delta R/R_0$ ) of the Ppy and COOH-Ppy micropattern electrode junctions, respectively. The collective sensing outcomes for individual organic vapors aggregate into distinct groups in the plot, thus providing signatures for the identification of different organic vapors. Compared to recently developed resistive sensors capable of detecting and identifying organic solvents,<sup>[19–21]</sup> this binary sensor exhibits superior sensitivity and negligible memory effects.

In conclusion, a novel electrochemical micropatterning technology, which utilizes a hydrodynamically focused laminar stream as a dynamic template, has been successfully demonstrated for site-specific fabrication of a sensor array composed of a number of intact Ppy- and functionalized Ppy-based micropatterns. The resulting array in a microfluidic device is a ready-to-use sensor capable of handling and detecting microliter amounts of organic solvent vapors (nanogram to microgram by weight). By employing two different sensing elements within the sensor array, the collective sensing responses are informative enough to identify a wide range of organic vapors. It is conceivable that this technology could be widely applied to micropatterning of other redox-active materials for broader application in microelectronic devices.

Received: September 15, 2007

Revised: October 27, 2007

Published online: January 4, 2008

**Keywords:** conducting materials · microfluidics · micropatterning · polymers · sensors

- [1] J. C. McDonald, G. M. Whitesides, *Acc. Chem. Res.* **2002**, *35*, 491–499.
- [2] M. Geissler, Y. N. Xia, *Adv. Mater.* **2004**, *16*, 1249–1269.
- [3] E. Menard, M. A. Meitl, Y. G. Sun, J. U. Park, D. J. L. Shir, Y. S. Nam, S. Jeon, J. A. Rogers, *Chem. Rev.* **2007**, *107*, 1117–1160.
- [4] A. J. Heeger, *Angew. Chem.* **2001**, *113*, 2660–2682; *Angew. Chem. Int. Ed.* **2001**, *40*, 2591–2611.
- [5] A. G. MacDiarmid, *Angew. Chem.* **2001**, *113*, 2649–2659; *Angew. Chem. Int. Ed.* **2001**, *40*, 2581–2590.
- [6] H. Shirakawa, *Angew. Chem.* **2001**, *113*, 2642–2648; *Angew. Chem. Int. Ed.* **2001**, *40*, 2574–2580.
- [7] J. M. Ziebarth, A. K. Saafir, S. Fan, M. D. McGehee, *Adv. Funct. Mater.* **2004**, *14*, 451–456.
- [8] C. Luo, R. Poddar, X. C. Liu, *J. Vac. Sci. Technol. B* **2006**, *24*, L19–L22.
- [9] J. A. Rogers, Z. N. Bao, V. R. Raju, *Appl. Phys. Lett.* **1998**, *72*, 2716–2718.
- [10] N. L. Jeon, I. S. Choi, B. Xu, G. M. Whitesides, *Adv. Mater.* **1999**, *11*, 946–950.
- [11] A. Baba, W. Knoll, *Adv. Mater.* **2003**, *15*, 1015–1019.
- [12] F. Zhou, M. Chen, W. M. Liu, J. X. Liu, Z. L. Liu, Z. G. Mu, *Adv. Mater.* **2003**, *15*, 1367–1370.
- [13] D. G. Shchukin, D. S. Kommireddy, Y. J. Zhao, T. H. Cui, G. B. Sukhorukov, Y. M. Lvov, *Adv. Mater.* **2004**, *16*, 389–393.
- [14] P. J. A. Kenis, R. F. Ismagilov, G. M. Whitesides, *Science* **1999**, *285*, 83–85.
- [15] J. U. Park, M. A. Meitl, S. H. Hur, M. L. Usrey, M. S. Strano, P. J. A. Kenis, J. A. Rogers, *Angew. Chem.* **2006**, *118*, 595–599; *Angew. Chem. Int. Ed.* **2006**, *45*, 581–585.
- [16] R. F. Ismagilov, A. D. Stroock, P. J. A. Kenis, G. Whitesides, H. A. Stone, *Appl. Phys. Lett.* **2000**, *76*, 2376–2378.
- [17] J. Atencia, D. J. Beebe, *Nature* **2005**, *437*, 648–655.
- [18] J. B. Knight, A. Vishwanath, J. P. Brody, R. H. Austin, *Phys. Rev. Lett.* **1998**, *80*, 3863–3866.
- [19] K. J. Albert, N. S. Lewis, C. L. Schauer, G. A. Sotzing, S. E. Stitzel, T. P. Vaid, D. R. Walt, *Chem. Rev.* **2000**, *100*, 2595–2626.
- [20] J. Janata, M. Josowicz, *Nat. Mater.* **2003**, *2*, 19–23.
- [21] M. C. McAlpine, H. Ahmad, D. W. Wang, J. R. Heath, *Nat. Mater.* **2007**, *6*, 379–384.
- [22] J. Wang, S. Chan, R. R. Carlson, Y. Luo, G. L. Ge, R. S. Ries, J. R. Heath, H. R. Tseng, *Nano Lett.* **2004**, *4*, 1693–1697.
- [23] J. Wang, Y. L. Bunimovich, G. D. Sui, S. Savvas, J. Y. Wang, Y. Y. Guo, J. R. Heath, H. R. Tseng, *Chem. Commun.* **2006**, 3075–3077.
- [24] Y. N. Xia, G. M. Whitesides, *Annu. Rev. Mater. Sci.* **1998**, *28*, 153–184.
- [25] M. J. Owen, P. J. Smith, *J. Adhes. Sci. Technol.* **1994**, *8*, 1063–1075.
- [26] J. C. McDonald, D. C. Duffy, J. R. Anderson, D. T. Chiu, H. K. Wu, O. J. A. Schueller, G. M. Whitesides, *Electrophoresis* **2000**, *21*, 27–40.
- [27] When one-step sheath-flow compression was applied to generate a focused stream with a width smaller than 4  $\mu\text{m}$ , the instability manifested in the form of shaky or discontinuous focused streams.
- [28] C. Mousty, B. Galland, S. Cosnier, *Electroanalysis* **2001**, *13*, 186–190.
- [29] G. W. Lu, C. Li, G. Q. Shi, *Polymer* **2006**, *47*, 1778–1784.
- [30] B. P. J. de Lacy Costello, P. Evans, N. Guernion, N. M. Ratcliffe, P. S. Sivanand, G. C. Teare, *Synth. Met.* **2000**, *114*, 181–188.